

A Low-cost Video-oculography System for Vestibular Function Testing

Jihwan Park, Youngsun Kong, Yunyoung Nam

Abstract— In order to remain in focus during head movements, vestibular-ocular reflex causes eyes to move in the opposite direction to head movement. Disorders of vestibular system decrease vision, causing abnormal nystagmus and dizziness. To diagnose abnormal nystagmus, various studies have been reported including the use of rotating chair tests and videonystagmography. However, these tests are unsuitable for home use due to their high costs. Thus, a low-cost video-oculography system is necessary to obtain clinical features at home. In this paper, we present a low-cost video-oculography system using an infrared camera and Raspberry Pi board for tracking the pupils and evaluating a vestibular system. Horizontal eye movement is derived from video data obtained from an infrared camera and infrared light-emitting diodes, and the velocity of head rotation is obtained from a gyroscope sensor. Each pupil was extracted using a morphology operation and a contour detection method. Rotatory chair tests were conducted with our developed device. To evaluate our system, gain, asymmetry, and phase were measured and compared with System 2000. The average IQR errors of gain, phase and asymmetry were 0.81, 2.74 and 17.35, respectively. We showed that our system is able to measure clinical features.

I. INTRODUCTION

During human locomotion, vision is disturbed by head perturbations [1]. The vestibulo-ocular reflex (VOR) helps the eyes fix on a target ahead, by rotating the moving eyes in the opposite direction [2]. This compensatory eye movement is induced by sensing angular acceleration in the semicircular canals of the vestibular system [3]. However, vestibular dysfunction in the form of blurring of vision in that a target slips from the fovea is called nystagmus [4]. Visual acuity can decrease by 50% when an object is only 2° from the center of the fovea [1]. From 2001 to 2004, 35.4% of US adults aged 40 or older had some degree of vestibular dysfunction [5].

To diagnose nystagmus and evaluate the semicircular canals, rotatory chair tests are conducted on suspected patients [6]. These tests include the sinusoidal harmonic acceleration (SHA) test and the velocity step test. The SHA test measures dizziness by rotating a chair with frequencies of 0.01- 0.64 Hz increased by two times in terms of sinusoidal velocity, and by measuring eye movement [6]. To analyze eye movement signals with the SHA test, three factors are calculated, which are gain, asymmetry, and phase. Each feature represents overall responsiveness, degree of symmetry between left and right stimuli, and time difference between head stimulus and eye movement.

Electronystagmography (ENG) measures movements of the eye by attaching electrodes around the nose, while ENG has the advantages of being able to make measurements while the eyes are closing, ENG has disadvantages of artifacts being caused by eye blinking, perspiration, or light, and difficulty in measuring vertical eye movement. Additionally, scleral search coil system (SSCS) requires subjects to insert an annular contact lens into their eyes; although having a high accuracy and sampling rate, it can be worn for only 40 min and has a tendency to slip [9,10]. With advances in computer vision technology, videonystagmography (VNG) has been used generally, although ENG data are still valuable [11]. VNG is a technology that can test whether dizziness is caused by inner ear disease; it uses an infrared camera to track the pupil in the dark. Advantages of VNG are its high accuracy and non-invasive nature, making its use common, although the high cost.

Various VNG studies have been conducted [12-14]. In [12], researchers suggested a new method to resolve the problem of estimating the eye position in VNG analysis brought about by deformable contour methods that are too slow for tracking eye movement by Otsu's thresholding for the detection of pupil areas and a snake-model for image segmentation. They suggested a method based on position, amplitude, and duration that could track saccade movement with high accuracy. In [13], a method of vestibular disease analysis for VNG applications was proposed, and new features were suggested based on Fisher's criteria for the diagnosis of nystagmus. To extract pupil, segmentation was applied using the Hough transform, and frequency variation of nystagmus was computed in fast and slow phase eye movement. In [14], researchers proposed a method for medical characteristics analysis with the displacement vectors of nystagmus using Gaussian mixture models (GMM). Video data were captured using infrared cameras and two-dimensional displacement vectors were calculated by comparing two adjacent frames. Then, GMM was applied to analyze the vectors. In this paper, a pair of head-mounted goggles was built with an infrared camera and used with a rotatory chair to conduct SHA tests.

Thus, a low-cost VNG system for SHA test was designed. Pupil coordination was extracted from the video data. From the pupil data, gain, phase, and asymmetry were calculated for measuring rapid eye movements. Finally, these factors were compared with System 2000 [15] results. The remainder of the paper is organized as follows. Section 2 describes the methods of the low-cost video-oculography system. In Section 3,

* This work was supported by the Soonchunhyang University Research Fund and was also supported by the Bio & Medical Technology Development Program of the NRF funded by the Korean government, MSIP(NRF-2015M3A9D7067219).

J. Park, Y. Kong and, Y. Nam are with the Department of Computer Science and Engineering, Soonchunhyang University, Asan 336-745, Korea (corresponding author to provide phone: +82-41-530-1282; fax: +82-41-530-1273; e-mail: ynam@sch.ac.kr).

experiments and results are presented. Finally, Section 4 discusses and provides conclusions.

II. METHODS

A. Prototype

As a prototype, head-mounted goggles were designed for obtaining eye movement signals. Figure 1 shows a pair of head-mounted goggles with an infrared camera and a gyroscope sensor. The goggles can record infrared videos of right eye of subject and measure rotatory velocity. To conduct a calibration, the participant can see the front with the left side of the goggles. The measured field of view is 32°. Three 850-nm infrared light-emitting diodes (LEDs) were attached to the goggles. To avoid noise caused by light reflexes, the LEDs were located at the bottom. The prototype consists of an infrared camera, a gyroscope sensor, and infrared LEDs. 3D virtual reality (VR) glasses (Maruneuru, Korea) [16] were used as the frame for the goggles. The Raspberry Pi 3 model B (Raspberry Pi Foundation, UK) [17] was used with the goggles for image processing and calculating features, due to its low cost, appropriate size, and fair image processing performance. Additionally, a Pi Camera (v2), equipped with a IMX219 8-megapixel sensor (Sony, Japan) [18], was used to evaluate infrared images of the eyes. A gyroscope MPU-6050 (InvenSense, USA) [19] was used to measure the velocity of the goggles.

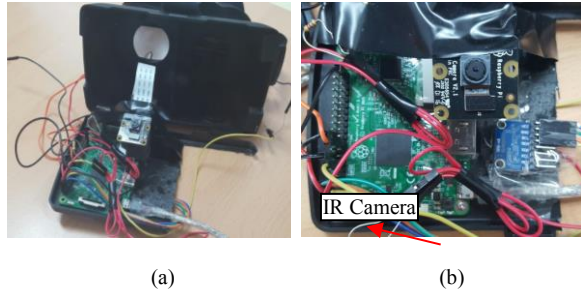


Figure 1. Head-mounted goggles with an infrared camera (a) goggles inside, (b) Raspberry Pi 3

B. Pupil Extraction

To obtain horizontal eye movement, the pupil was extracted from video data obtained with the goggles and the System 2000. Because pupils have a generally circular shape, the same method was used to both video data obtained from the goggles and the System 2000 with different threshold values of brightness and pupil size. The method includes noise removal and a circle-detection algorithm.

Figure 2 shows examples of pupil images obtained from an infrared camera. First, the gray channel was extracted with region-of-interest (ROI) selection from the infrared images for efficient image process. The sizes of the ROIs for the developed goggles and the System 2000 were set at 200×210 and 400×200 , respectively. Then, the intensity of the pupil area is higher than that of rest; thus, binary images were obtained from the extracted gray channel. Binary images may contain noise caused by occlusion by the eyelids and eyelashes. To solve the noise issue, a morphology operation

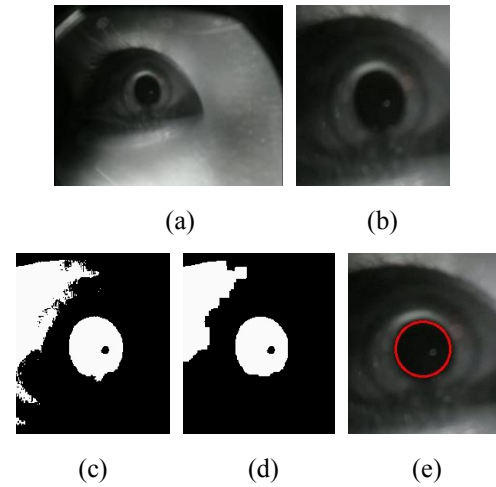


Figure 2. Example of pupil images (a) raw image, (b) selected ROI, (c) binarization, (d) morphology, (e) result of extracted pupil

was implemented. Finally, FindContours function in OpenCV library was applied to detect a circular region. Pupil among the detected contours was selected as follows:

$$\begin{aligned} \text{abs}\left(1 - \frac{w}{h}\right) &< k, \\ \text{abs}\left(1 - \frac{s}{\pi \cdot \left(\frac{w}{2}\right)^2}\right) &< k, \end{aligned}$$

,where w , h and s represent width, height and area of detected contours, respectively; and k represents a constant value which was set to 0.6 or more. The minimum radius and area of the detected circle were set to 20 and 30, respectively.

C. Slow Phase Eye Movement

Figure 3 shows part of the eye movement signal obtained from System 2000. The dashed rectangles and the solid rectangles indicate fast-phase and slow-phase eye movement, respectively. To extract gain, asymmetry, and phase from eye-movement signals, the slow phase velocity of the pupil should be calculated [1].

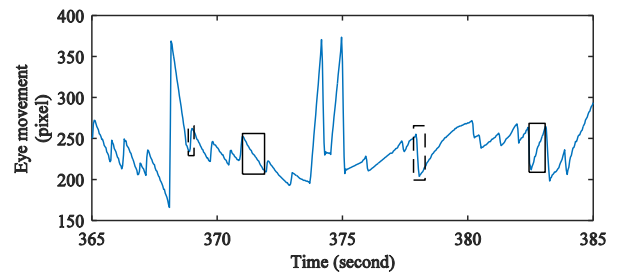


Figure 3. Pupil movement signal

Slow phase velocity is derived from raw signal as follows. First, the horizontal pupil movement signal was extracted from the infrared video data using a pupil extraction method. Missing frames caused by eye blinking were set as negative numbers. In compensating for missing frames caused by eye blink artifacts, a linear spline algorithm was implemented. Moreover, a cubic spline algorithm was implemented to interpolate the signal to 30 Hz due to the irregular sampling rate (27–29 fps). Pupil velocity was also derived from the interpolated signal.

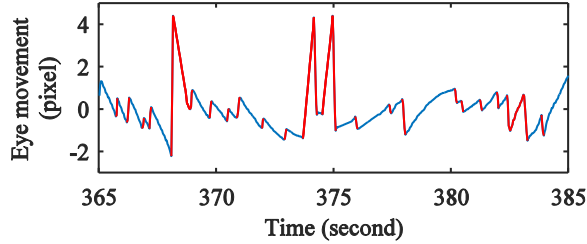


Figure 4. Obatined fast phase

The fast phase of the signal was removed as follows. Since having a larger slope than the slow-phase velocity, the fast-phase velocity was determined based on slope degree. Normalization, differentiator, and squaring operations were used. Then, the eye movement signal was derived and squared, to obtain the slope of the signal. Peaks were detected by a threshold value from the squared signal, which were manually set based on each velocity of chair. As shown in Figure 4, the red line represents the fast phase obtained. Finally, the fast phase was removed from the derived signal.

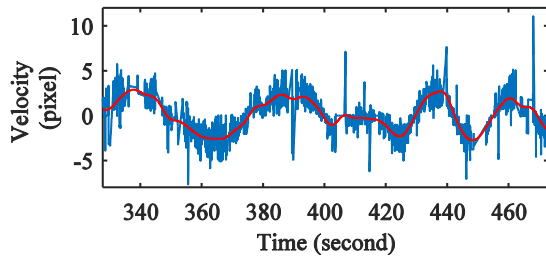


Figure 5. Obatined Slow phase and lowpass filter

After the fast phase signal was eliminated, a linear spline algorithm was used. As shown in Figure 5, low-pass filter was applied to remove noise.

D. Gain, Asymmetry and Phase

Gain is the ratio of the amplitude of the eye movement to the amplitude of head stimulus [20]. Symmetry is indicated by comparable left and right responses when the same stimulus is applied [20]. Phase is the timing relationship between the initiation of head movement and the reflexive eye response [20]. Gain, symmetry and phase are calculated as follows:

$$\text{Gain} = \frac{\text{Amplitude of the maximum slow phase eye velocity}}{\text{Amplitude of the maximum stimulus velocity}},$$

$$\text{Symmetry} = \frac{b_2 - b_1}{b_2 + b_1} \times 100,$$

$$\text{Phase } (\varphi^\circ) = 360^\circ \cdot f \cdot \Delta t,$$

where b_1 and b_2 represent the maximum velocity of slow-phase eye movement in rotating to the left and right, respectively; f represents the frequency of the eye movement signal and Δt represents the time difference between the maximum velocity of slow-phase eye movement and head movement.

III. RESULTS

A. Experiments

Data were collected from eight healthy non-smoking men and two women aged from 20 to 28 years. All subjects wore the developed goggles and System 2000 goggles, while seated on a rotatory chair (System 2000) in the sitting position. Each experiment was performed seven times for each frequency. The chair was rotated with maximum velocity from 80° to 20° for 2-8 cycles. The videos from the goggles were recorded at 600×420 resolution. The videos from the System 2000 were obtained using the built-in camera on a Galaxy S6 (Samsung, Korea) at 1920×1080 resolution, because no video data are ordinarily provided by the System 2000. Both video data were recorded at 30 Hz.

B. Results

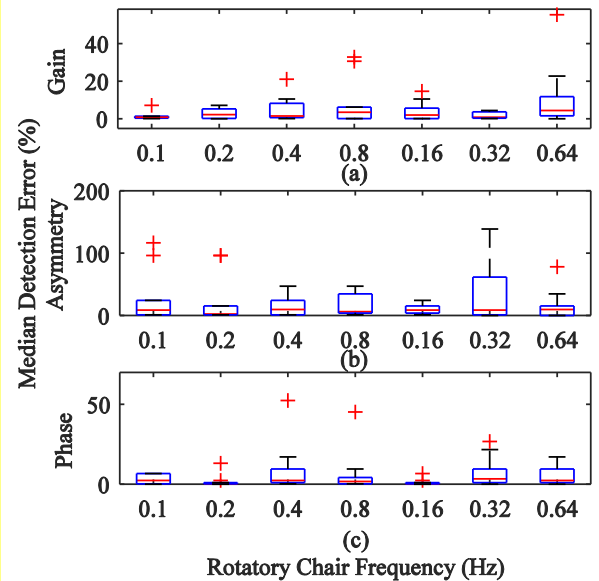


Figure 6. Medain and IQR errors measured from the (a) gain, (b) asymmetry and (c) phase at each frequency

To evaluate the results, we calculated the error ε for each frequency of gain, phase, and asymmetry, as follows:

$$\varepsilon = \frac{\text{mean}(\text{abs}(x - x_{\text{est}}))^2}{\text{mean}(\text{abs}(x))^2},$$

where x and x_{est} represent the reference and estimated feature, respectively. Each error for gain, phase, and asymmetry were measured among all subjects for each frequency. Figure 6 shows the median and interquartile range (IQR) of the errors measured from the results at each frequency. The average errors of gain, asymmetry, and phase were 0.81, 17.35, and 2.74, respectively.

IV. CONCLUSION AND DISCUSSION

This paper has presented a low-cost VNG using an infrared camera for the diagnosis of nystagmus by obtaining eye movement features. The device was developed using a pair of head-mounted goggles, a Raspberry Pi board, an infrared camera, and LEDs. To extract and track the pupil from video data obtained from the device, a morphology operation and a contour detection method were used. The miss rate when applying the morphology operation was 18.54%, whereas without applying it, the rate was 66.9%. The horizontal eye movement signal was obtained and its slow-phase velocity was calculated. Accordingly, the average IQR errors of gain and phase were 0.81 and 2.74, while that of asymmetry was 17.35.

Interpolation algorithms were used to detect missing signals caused by eye blinking in the subjects. Also, video data for the System 2000 were not captured exactly in front of the monitor and had minor oscillation noise caused by movements of subjects. Accordingly, the average error of asymmetry were larger than those of gain and phase.

Some images were not detected due to noise caused by occlusion by eyelids and eyelashes. Additionally, the number, location, and wavelength of the LEDs were not verified in the experiments. Moreover, the developed goggles were not evaluated with a clinical device, because it is hard to use two sets of goggles simultaneously without generating noise. More experiments are needed for clinical tests. We will evaluate the goggles using the velocity step test and compare between the goggles and other clinical equipment.

ACKNOWLEDGMENT

The authors would like to thank Namik Kim and Hyeonsoo Lee for their valuable contribution to this project.

REFERENCES

- [1] R. J. Leigh and D. S. Z. M.D., *The Neurology of Eye Movements*. Oxford University Press, 2015.
- [2] R. W. Ditchburn and B. L. Ginsborg, "Involuntary eye movements during fixation," *J Physiol*, vol. 119, no. 1, pp. 1–17, Jan. 1953.
- [3] J. L. Meiry, "The vestibular system and human dynamic space orientation," Thesis, Massachusetts Institute of Technology, 1965.
- [4] J. M. Epley, "Positional Vertigo Related to Semicircular Canalithiasis," *Otolaryngol Head Neck Surg*, vol. 112, no. 1, pp. 154–161, Jan. 1995.
- [5] Y. Agrawal, J. P. Carey, C. C. D. Santina, M. C. Schubert, and L. B. Minor, "Disorders of Balance and Vestibular Function in US Adults: Data From the National Health and Nutrition Examination Survey, 2001–2004," *Arch Intern Med*, vol. 169, no. 10, pp. 938–944, May 2009.
- [6] T. Hain, "Rotatory Chair Testing", Dizziness-and-balance.com, 2016. [Online]. Available: <http://www.dizziness-and-balance.com/testing/ENG/rchair.html>.
- [7] J. Lb, "[ELECTRONYSTAGMOGRAPHY]," *HNO*, vol. 12, pp. 325–329, Dec. 1964.
- [8] D. A. Robinson, "A Method of Measuring Eye Movement Using a Scleral Search Coil in a Magnetic Field," *IEEE Transactions on Bio-medical Electronics*, vol. 10, no. 4, pp. 137–145, Oct. 1963.
- [9] S. T. Moore, T. Haslwanter, I. S. Curthoys, and S. T. Smith, "A geometric basis for measurement of three-dimensional eye position using image processing," *Vision Res.*, vol. 36, no. 3, pp. 445–459, Feb. 1996.
- [10] T. Imai *et al.*, "Comparing the accuracy of video-oculography and the scleral search coil system in human eye movement analysis," *Auris Nasus Larynx*, vol. 32, no. 1, pp. 3–9, Mar. 2005.
- [11] M. M. Ganança, H. H. Caovilla, and F. F. Ganança, "Electronystagmography versus videonystagmography," *Brazilian Journal of Otorhinolaryngology*, vol. 76, no. 3, pp. 399–403, Jun. 2010.
- [12] A. B. Slama, A. N. Machraoui, and M. Sayadi, "Pupil tracking using active contour model for videonystagmography applications," in *International Image Processing, Applications and Systems Conference*, 2014, pp. 1–5.
- [13] A. B. Slama *et al.*, "Features extraction for medical characterization of nystagmus," in *2016 2nd International Conference on Advanced Technologies for Signal and Image Processing (ATSIP)*, 2016, pp. 292–296.
- [14] Y. Mao, Q. Wang, J. Miao, and W. He, "An application of Gaussian mixture models for medical characteristics analysis of nystagmus signals," in *2013 6th International Conference on Biomedical Engineering and Informatics*, 2013, pp. 18–23.
- [15] System 2000. Micromedical. <http://www.micromedical.com/Products/Rotational-Chairs/>
- [16] Lx130 3D VR Glasses. Marunuru. <http://maruit.com/>
- [17] Raspberry Pi 3 model B. Raspberry PI Foundation. <https://www.raspberrypi.org/products/raspberry-pi-3-model-b/>
- [18] IMX219. Sony. http://www.sony-semicon.co.jp/products_en/new_pro/april_2014/imx219_e.html
- [19] MPU-6050. InvenSense. <https://www.invensense.com/products/motion-tracking/6-axis/mpu-6050/>
- [20] J. M. Goldberg, *The Vestibular System: A Sixth Sense*. OUP USA, 2012.